

# Buckling load analysis of cracked curved beams using differential quadrature element method

M. Zare<sup>1</sup>, A. Asnafi<sup>2\*</sup>

<sup>1</sup>Department of Mechanical Engineering, Shahid Chamran University, Ahvaz, 61355, Iran.

<sup>2</sup>Hydro-Aeronautical Research Center, Shiraz University, Shiraz, 71348-51154, Iran.

## ABSTRACT

This paper investigated the buckling load of a cracked curved beam subjected to external excitations considering the effects of shear deformations and geometric nonlinearity due to large deformations. The governing nonlinear equations of motion were derived. The analysis in stationary case was developed for each half of the beam and then the differential quadrature element method (DQEM) was used to discretize and solve the problem. The resulting nonlinear system of equation was analyzed using continuity conditions between the beam segments and an arc length strategy. To verify the validity of the proposed method, the beam was modeled using the finite element method. The agreement between the results showed the accuracy of the proposed method in prediction the buckling load of the beam. Finally, the effect of crack parameters (depth and location) on the buckling load was investigated. As the results showed, the crack depth and buckling load related conversely. Furthermore, the closer the crack to the midpoint, the less load was required to make the beam undergo buckling.

**KEYWORDS:** Differential quadrature element method (DQEM), Curved beam vibration, Buckling load, Arc length method, Non-linear analysis.

## 1.0 INTRODUCTION

Curved beams have been applied in a variety of industries to be used as mechanical devices, building arches and so on. Obviously, over time, such structures can be damaged and one of the most prevalent damages is crack. Moreover, the stability of structures is of high significance; so, it is a great idea to have a deeper insight into the stability analysis of cracked structural elements.

Much research has been done about the stability of beams as well as their damage phenomena. Bradford et al. (Bradford, 2002) studied the in-plane elastic stability of arches under a central concentrated load analytically. The stability of a cracked beam exited by a follower load was done by Wang (Wang, 2004). In that research, the critical load was obtained on the basis of the variation of resonant frequencies. In-Soo et al (Son, 2007) studied the natural frequencies of a cracked beam exposed to a follower force. In their study the buckling load of the beam was also calculated. The static stability analysis of a uniform column with multiple cracks has been done by Caddemi et.al (Caddemi,

---

\*Corresponding Author. Email: [asnafi@shirazu.ac.ir](mailto:asnafi@shirazu.ac.ir)

2013). In that research the buckling modes as well as the corresponding buckling loads were presented. In another study done by Nikpour (Nikpour, 1990), the buckling phenomenon of a beam with an edged-notched composite was analyzed. In the mentioned study, the local compliance due to the crack was considered as a function of the crack-tip stress intensity factors and the elastic properties of material. The buckling and post buckling analysis of curved beams under distributed, concentrated and thermal loads were done by Eslami (Eslami, 2018). In that study, different boundary conditions and loads were studied and then the pre and post buckling loads of rings were obtained and discussed. Attard (Attard, 1986) presented two new finite element formulations for obtaining the lateral buckling load of elastic beams under static loads. Torabi et al. (Torabi, 2014) studied the free vibration of a Timoshenko beam with multiple cracks using differential quadrature element method (DQEM). In that study, they revealed that how crack parameters influenced the natural frequencies.

In this study the buckling load of a general cracked curved beam with a radial concentrated force at middle point of the beam is investigated. The problem is solved considering the static analysis based on the differential quadrature element and arc length methods and finally, a formula is proposed for the buckling load with respect the radial displacement of the mid-point of the beam. Also, the effect of crack parameters, depth and location, on the buckling load is studied.

## 2.0 EQUATION OF MOTION OF THE CRACKED CURVED BEAM

The equations of motion for a curved beam's post-buckled state, taking into account the effects of shear deformation and rotary inertia, as well as, the extension of the neutral axis, can be written as (Nikpour, 1990):

$$N\left(\frac{1}{R} - \frac{\partial\varphi}{\partial S}\right) - \frac{\partial Q}{\partial S} = -\gamma A \ddot{u} \quad (1)$$

$$Q\left(\frac{1}{R} - \frac{\partial\varphi}{\partial S}\right) + \frac{\partial N}{\partial S} = \gamma A \ddot{v} \quad (2)$$

$$\frac{\partial M}{\partial S} - N\frac{Q}{kAG} + Q\left(\frac{N}{EA} + 1\right) = \gamma A \ddot{w} \quad (3)$$

$$\frac{N}{EA} = \left(\left(\frac{\partial U}{\partial S} + \frac{W}{R} + 1\right)\cos(\varphi) + \left(\frac{\partial W}{\partial S} - \frac{U}{R}\right)\sin(\varphi) - 1\right) \quad (4)$$

$$\frac{Q}{kAG} = \left(-\left(\frac{\partial U}{\partial S} + \frac{W}{R} + 1\right)\sin(\varphi) + \left(\frac{\partial W}{\partial S} - \frac{U}{R}\right)\cos(\varphi)\right) \quad (5)$$

$$M = EI \frac{\partial\varphi}{\partial S} \quad (6)$$

where dot means the derivative with respect to time. As shown in Fig. 1, which represents an element of a curved beam,  $W$ ,  $U$  and  $\varphi$  denote the radial and tangential displacements and the angle of rotation.  $M$ ,  $N$  and  $Q$  represent the bending moment, normal and shear distributed forces respectively. Moreover,  $A$ ,  $I$ ,  $\gamma$ ,  $G$ ,  $E$  and  $k$  are the structural properties of the beam, which denote area and moment of inertia of the cross section, mass density per unit volume of the beam material, shear and Young's modulus, and shear factor of the cross section, respectively. In this figure  $\beta$  is the angular location of the crack.

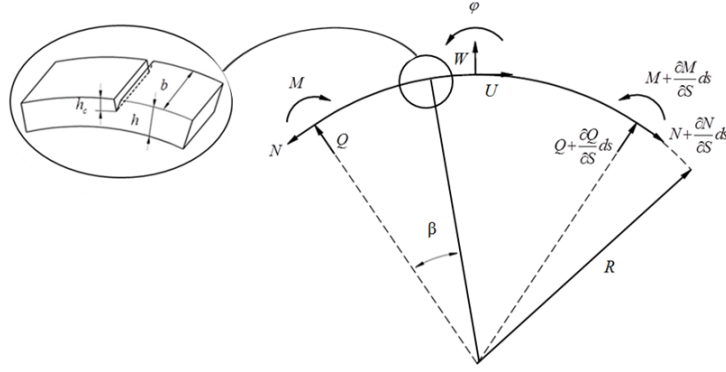


Figure 1. Load and displacement components of a curved beam element (Karaagac, 2011)

In order to include the effect of crack, a rotational spring with stiffness ( $K_0$ ) is assumed as (Cerri, 2008):

$$K_0 = \frac{EI^D}{(EI - EI^D) h / \alpha}, EI^D = E \frac{1}{12} b(h - h_c)^3, EI = E \frac{1}{12} (bh^3) \quad \alpha \approx \quad (7)$$

The equations of motion are solved by DQE method which is a new numerical method for rapidly solving linear and nonlinear differential equations (Appendix A).

At equilibrium state, the terms containing time evolutions in Eqs. (1-6) are eliminated. Then, by applying DQ discretization to the equations of motion at an interior node  $m^i$ , in an element  $i$ , the following equilibrium equations are obtained:

$$(N_{m^i}^i)_e \left( \frac{1}{R} - \frac{\partial(\varphi_{m^i}^i)_e}{\partial S} \right) - \frac{\partial(Q_{m^i}^i)_e}{\partial S} = 0 \quad (8)$$

$$(Q_{m^i}^i)_e \left( \frac{1}{R} - \frac{\partial(\varphi_{m^i}^i)_e}{\partial S} \right) + \frac{\partial(N_{m^i}^i)_e}{\partial S} = 0 \quad (9)$$

$$\frac{\partial(M_{m^i}^i)_e}{\partial S} - (N_{m^i}^i)_e \frac{(Q_{m^i}^i)_e}{KAG} + (Q_{m^i}^i)_e \left( \frac{(N_{m^i}^i)_e}{EA} + 1 \right) = 0 \quad (10)$$

$$\frac{(N_{m^i}^i)_e}{EA} - \left( \frac{\partial(U_{m^i}^i)_e}{\partial S} + \frac{(W_{m^i}^i)_e}{R} + 1 \right) \cos((\varphi_{m^i}^i)_e) + \left( \frac{\partial(W_{m^i}^i)_e}{\partial S} - \frac{(U_{m^i}^i)_e}{R} \right) \sin((\varphi_{m^i}^i)_e) - 1 = 0 \quad (11)$$

$$\frac{(Q_{m^i}^i)_e}{KAG} - \left( - \left( \frac{\partial(U_{m^i}^i)_e}{\partial S} + \frac{(W_{m^i}^i)_e}{R} + 1 \right) \sin((\varphi_{m^i}^i)_e) + \left( \frac{\partial(W_{m^i}^i)_e}{\partial S} - \frac{(U_{m^i}^i)_e}{R} \right) \cos((\varphi_{m^i}^i)_e) \right) = 0 \quad (12)$$

$$(M_{m^i}^i)_e - EI^i \frac{\partial(\varphi_{m^i}^i)_e}{\partial S} = 0 \quad (13)$$

Now, the continuity conditions are applied to each interface of the discretized segments of the beam. The continuity conditions make some relations between the radial and tangential displacements, the angular rotation, the normal and shear forces and the bending moment of adjacent elements.

The radial and tangential displacements and the angular rotation continuity conditions at the inter-element boundary of two adjacent elements  $i$  and  $i + 1$ , except for the crown of the beam and the cracked section, are expressed as:

$$W_{N^i}^i = W_1^{i+1}, U_{N^i}^i = U_1^{i+1}, \varphi_{N^i}^i = \varphi_1^{i+1} \quad (14)$$

In addition, the normal and shear forces and the bending moment continuity conditions at the inter-element boundary of two adjacent elements  $i$  and  $i + 1$  can be expressed, respectively, as:

$$E^i A^i \left( \left( \frac{\partial u_{N^i}^i}{\partial S} + \frac{w_{N^i}^i}{R} + 1 \right) \cos(\varphi_{N^i}^i) + \left( \frac{\partial w_{N^i}^i}{\partial S} - \frac{u_{N^i}^i}{R} \right) \sin(\varphi_{N^i}^i) - 1 \right) =$$

$$E^{i+1} A^{i+1} \left( \left( \frac{\partial u_1^{i+1}}{\partial S} + \frac{w_1^{i+1}}{R} + 1 \right) \cos(\varphi_1^{i+1}) + \left( \frac{\partial w_1^{i+1}}{\partial S} - \frac{u_1^{i+1}}{R} \right) \sin(\varphi_1^{i+1}) - 1 \right) \quad (15)$$

$$k^i A^i G^i \left( - \left( \frac{\partial u_{N^i}^i}{\partial S} + \frac{w_{N^i}^i}{R} + 1 \right) \sin(\varphi_{N^i}^i) + \left( \frac{\partial w_{N^i}^i}{\partial S} - \frac{u_{N^i}^i}{R} \right) \cos(\varphi_{N^i}^i) \right) =$$

$$k^{i+1} A^{i+1} G^{i+1} \left( - \left( \frac{\partial u_1^{i+1}}{\partial S} + \frac{w_1^{i+1}}{R} + 1 \right) \sin(\varphi_1^{i+1}) + \left( \frac{\partial w_1^{i+1}}{\partial S} - \frac{u_1^{i+1}}{R} \right) \cos(\varphi_1^{i+1}) \right) \quad (16)$$

$$E^i I^i \frac{\partial \varphi_{N^i}^i}{\partial S_{N^i}^i} = E^{i+1} I^{i+1} \frac{\partial \varphi_1^{i+1}}{\partial S_1^{i+1}} \quad (17)$$

The continuity conditions at the crown of the arch in the equilibrium state are:

$$U_{N^i}^i = U_1^{i+1}, \varphi_{N^i}^i = \varphi_1^{i+1}, W_{N^i}^i = w_0, W_1^{i+1} = w_0$$

$$\frac{\partial u_{N^i}^i}{\partial S} = \frac{\partial u_1^{i+1}}{\partial S}, \frac{\partial \varphi_{N^i}^i}{\partial S} = \frac{\partial \varphi_1^{i+1}}{\partial S}, i = \frac{m}{2} \quad (18)$$

where,  $w_0$  is the radial displacement of the middle point of the beam. Also, the continuity conditions at the cracked section is:

$$W_{N^i}^i = W_1^{i+1}, U_{N^i}^i = U_1^{i+1}, K_0(\varphi_{N^i}^i - \varphi_1^{i+1}) = M_c \quad (19)$$

Where  $M_c$  is the bending moment at the cracked section. Finally, the boundary conditions for a beam clamped at both ends are:

$$W_1^1 = 0 \quad \varphi_1^1 = 0 \quad U_1^1 = 0 \quad (20)$$

$$W_{N^m}^m = 0 \quad \varphi_{N^m}^m = 0 \quad U_{N^m}^m = 0 \quad (21)$$

To compute the buckling load, the radial displacement of the crown of the beam ( $w_0$ ) is used as the input of the arc length strategy to obtain the concentrated load in each half of the arch. In this manner, by investigation the normal force  $N$ , shear force  $Q$ , and the angular rotation  $\varphi$  at the arch crown, the concentrated load in each half of the beam is calculated as (Zhu, 2014):

$$F_1 = N_N^i \sin(\varphi_N^i) + Q_N^i \cos(\varphi_N^i), \quad F_2 = N_1^{i+1} \sin(\varphi_1^{i+1}) + Q_1^{i+1} \cos(\varphi_1^{i+1}) \quad (22)$$

Now, by applying the continuity conditions at the crown point of the beam, the value of buckling force is obtained as:

$$P_c = |F_1 - F_2|, \quad i = \frac{m}{2} \quad (22)$$

### 3.0 RESULTS AND DISCUSSION

Without any loss of generality, using Eqs. (22 & 23), the magnitude of the concentrated load versus the radial displacement of the middle point ( $w_0$ ), for a clamped-clamped beam with the properties of Table.1 was obtained and plotted in Fig. 2. It is to be noted that to ensure about the accuracy of the proposed method, a finite element simulation was also done and the results obtained throughout above methods were compared.

Table 1. Mechanical properties of the curved beam

Property	Notation	Value
Radius of the beam axis	$R$	83 (cm)
Opening angle of the beam	$\theta$	40 (deg)
Height of the cross section	$h$	0.5 (cm)
Base of the cross section	$b$	2 (cm)
Young's Modulus	$E$	11 (GPa)
Poisson's Ratio	$\nu$	0.3
Density	$\gamma$	7800 (kg/m <sup>3</sup> )

A good agreement between the results obtained by our model and those obtained through FE modeling (ANSYS) was seen (see Fig. 2) which confirmed the accuracy of the proposed method.

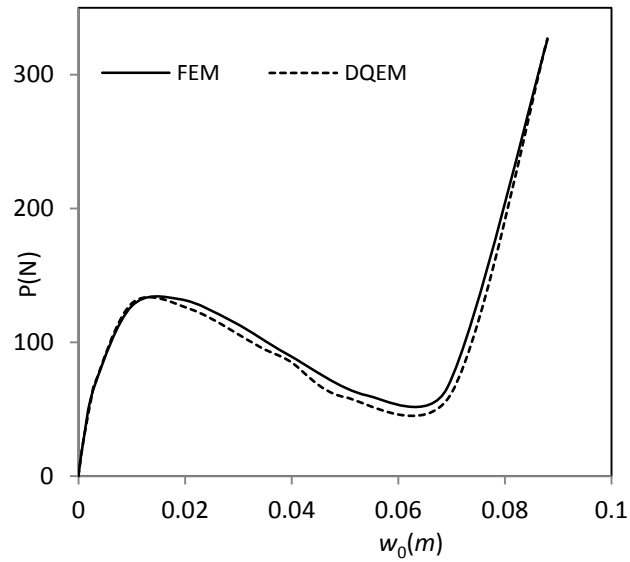


Figure 2. Variation of the concentrated load versus the crown radial displacement

Note also that in the FE simulation, the 3-node element BEAM189 was used to mesh and analyze the nonlinear buckling behavior of the beam. In the analysis, 100 elements were used to achieve more accurate results. See the finite element model along with the structured meshes in Fig.3.

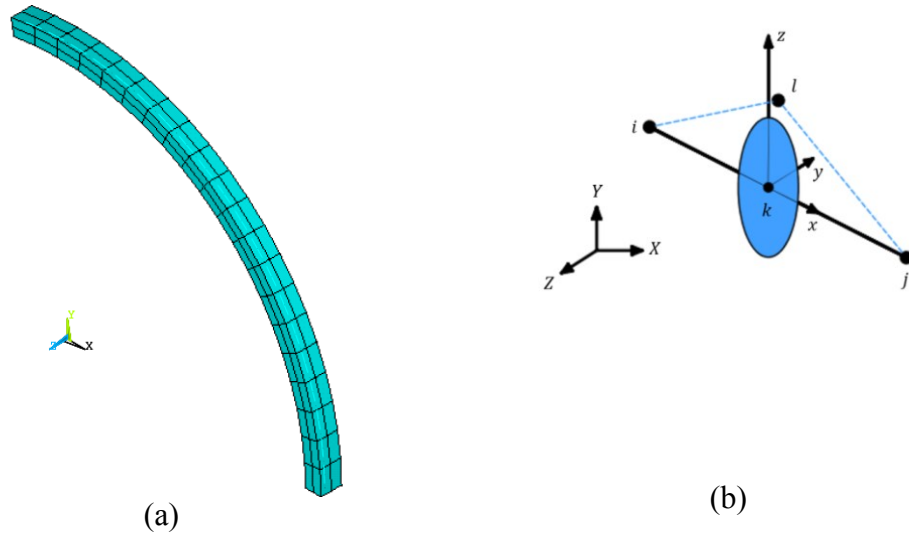


Figure 3. a: The finite element model of the beam. b: Assumed element for meshing the model

### 3.1 The effect of crack depth on the buckling load

In Fig. 4, the changing of the buckling load for the beam introduced in Table. 1 by a variation in the crack depth was shown. In this figure the relative location of the crack (the proportion of the angular location of the crack to the opening angle of the beam) is 0.17. Note that in this figure the relative depth is defined as the crack depth to the height of the cross section.

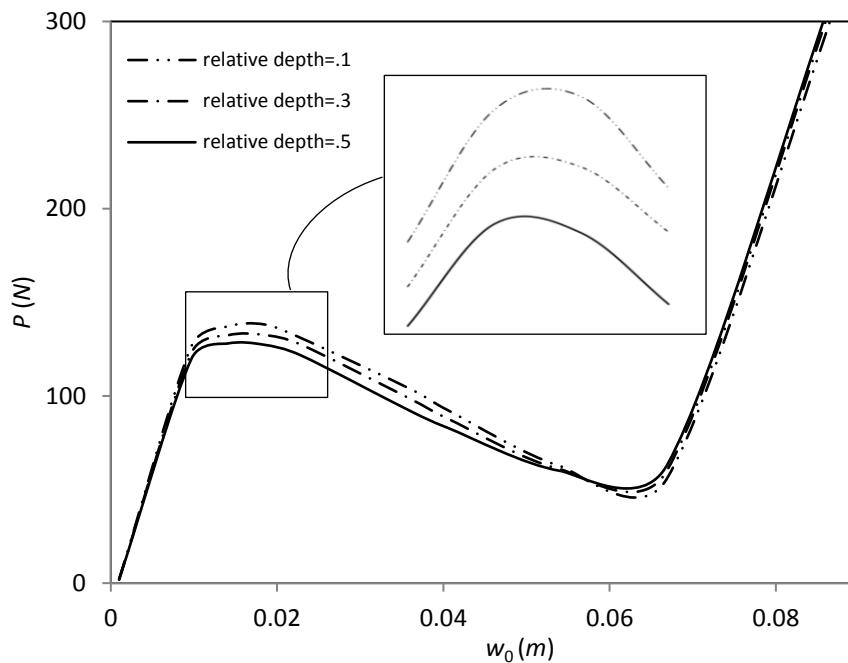


Figure 4. Changing of the buckling load versus the midpoint displacement for different crack depths

As the figure shows, increasing the crack depth make a decrease in the buckling load which is due to the decrease in the flexural stiffness of the beam.

### 3.2 The effect of crack location on the buckling load

In Fig.5, it is shown how the buckling load changes with the variation of the crack location for the aforementioned beam with relative crack depth of 0.5. It represents that as the crack location gets closer to the middle point of the beam, the buckling load decreases. This is mainly because the bending moment increases by moving toward the midpoint of the beam. Also, the crack effect is related to the bending moment as Eq.(19) shows; so, the buckling load decreases.

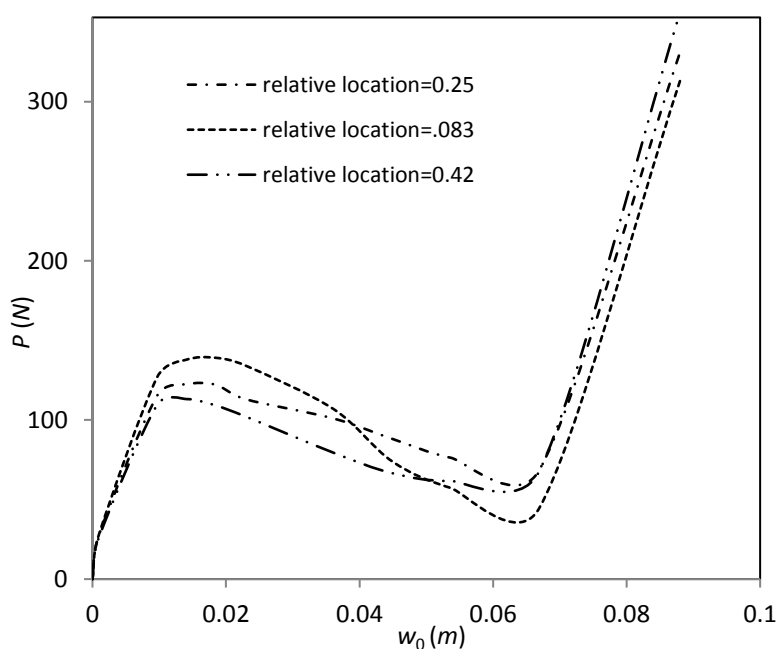


Figure 5. Changing of the buckling load versus the midpoint displacement for different crack locations

## 4.0 CONCLUSION

The differential quadrature element method along with an arc length strategy were used to obtain the buckling load of a cracked curved beam in this article. Using the equation of motion in stationary case, and applying the continuity conditions between adjacent segments of the beam, a formula for buckling load was proposed. The proposed method was firstly validated by a finite element simulation. After that, the effects of the crack depth and location on the buckling load were studied. It was shown that the buckling load became smaller as the depth of the crack increased or the crack location approached to the beam crown.

## 5.0 CONFLICT OF INTEREST

We declare that we have no conflict of interest.

## 6.0 REFERENCES

- Attard, M. M. (1986). Lateral buckling analysis of beams by the FEM. *Computers & structures*, 23(2), 217-231.
- Bradford, M. A. (2002). In-plane elastic stability of arches under a central concentrated load. *Journal of engineering mechanics*, 128(7), 710-719.
- Caddemi, S. C. (2013). The influence of multiple cracks on tensile and compressive buckling of shear deformable beams. *International Journal of Solids and Structures*, 50(20-21), 3166-3183.
- Cerri, M. N. (2008). Vibration and damage detection in undamaged and cracked circular arches: experimental and analytical results. *Journal of sound and vibration*, 314(1-2), 83-94.
- Eslami, M. R. (2018). Buckling and Post-buckling of Curved Beams and Rings. In *Buckling and Postbuckling of Beams, Plates, and Shells* (pp. 11-188). Springer.
- Karaagac, C. O. (2011). Crack effects on the in-plane static and dynamic stabilities of a curved beam with an edge crack. *Journal of Sound and Vibration*, 330(8), 1718-1736.
- Nikpour, K. (1990). Buckling of cracked composite columns. *International Journal of Solids and Structures*, 26(12), 1371-1386.
- Son, I. S. (2007). Stability Analysis of Cracked Cantilever Beam with Tip Mass and Follower Force. *Transactions of the Korean Society for Noise and Vibration Engineering*, 17(7), 605-610.
- Torabi, K. A. (2014). A DQEM for transverse vibration analysis of multiple cracked non-uniform Timoshenko beams with general boundary conditions. *Computers & Mathematics with Applications*, 6(3), 527-541.
- Wang, Q. (2004). A comprehensive stability analysis of a cracked beam subjected to follower compression. *International Journal of Solids and Structures*, 41(18-19), 4875-4888.
- Zhu, J. A. (2014). In-plane nonlinear buckling of circular arches including shear deformations. *Archive of Applied Mechanics*, 84(12), 1841-1860.

## APPENDIX A. DIFFERENTIAL QUADRATURE ELEMENT METHOD

The DQEM is a new numerical method for rapidly solving linear and nonlinear differential equations. The DQEM is based on the DQ method, an approximate method for expressing partial derivatives of a function at a point located in the domain of the function, as the weighted linear sum of the values of the variable function at all the defined precision points in the derivation direction. Eq. (A.1) is the mathematical representation of the DQ expansion:

$$\frac{df}{dx} \Big|_{x=x_i} = \sum_{j=1}^N C_{ij}^{(1)} f_j \quad i, j = 1, 2, 3, \dots, N \quad (\text{A.1})$$

where  $f$  is the function,  $N$  is the number of precision points,  $x_i$  is the precision associated with the  $i$ -th point of the function domain, and represents the weighting coefficients used for finding the first derivative of the function at the  $i$ -th precision point of the function domain represented as  $x_i$  above. In the DQEM, the studied structure is divided into several elements. Then, the continuity conditions are applied on the inter-element boundary of two adjacent elements and the boundary conditions of the beam as well as the governing equations on each element, using the differential quadrature method. According to Eq. (A.1), two important factors in the DQ method include: calculation of the DQ weighting coefficients, and selecting the precision points. The Lagrangian functions were used to compute the weighted coefficients, and the Gauss–Lobatto Chebyshev polynomial was used for selecting the precision points.